The synthesis of novel, visible-wavelength oxidizable polymerization sensitizers based on the 5,12-dihydroquinoxalino[2,3-b]pyridopyrazine skeleton

Radosław Podsiadły*

Institute of Polymer and Dye Technology, Technical University of Lodz, Stefanowskiego 12/16, 90-924 Lodz, Poland

ARTICLE INFO

ABSTRACT

Novel dyes based on the 5,12-dihydroquinoxalino[2,3-b]pyridopyrazine skeleton were synthesized and subsequently characterized using ^{1}H NMR. Their electrochemical and spectral properties, such as absorption and emission spectra, quantum yield of fluorescence, and quantum yield of singlet oxygen generation, were also measured. The dyes were useful as photoinitiators for sensitizing compounds to photooxidation. Photoredox pairs comprising dyes and onium salts were found to be effective visible-wavelength initiators of free radical or cationic polymerization.

© 2008 Elsevier Ltd. All rights reserved.

1. Introduction

Light-induced photopolymerization has several advantages over other comparable methods. For instance, the process is low-temperature and can be controlled by manipulating the intensity and wavelength of the radiation source. Both free radical and cationic polymerizations are generally restricted to certain types of monomers. Many olefinic and acrylic monomers undergo photo-initiated free radical polymerization, while epoxides and vinyl ethers are solely polymerizable via cationic mechanisms [1].

Many early radiation-based systems for initiating free radical or cationic polymerization reactions respond to UV light. In these free radical photopolymerization reactions, UV-absorbing compounds undergo fragmentation directly following photonic excitation to form the free radical initiator species. As an example, the UV-induced fragmentation of benzoin aryl ether is depicted in Scheme 1 [2]. In cation-induced polymerization reactions, photolysis initiators undergo irreversible photofragmentation in response to UV excitation to produce free radical, cationic, and radical cation fragments. The aryl cations and aryliodine radical cations generated from photolysis further react with either solvent molecules or monomers to generate strong protic acid, H^+X^-, which, in turn, initiates the polymerization of monomers. As an example, the

UV-induced ionic fragmentation of an iodonium salt and the subsequent acid formation are presented in Scheme 2 [3].

Onium salts used in cationic photopolymerization primarily absorb wavelengths of light between 225 and 350 nm. In order to extend the spectral sensitivity of these initiators to the visible light, sensitizers are used. The most efficient and generally applicable mechanism of photosensitization of diaryliodonium [4], triphenylsulfonium [5], and N-alkoxypyridinium [6] salts is photoinduced intermolecular electron transfer processes. In such sensitization processes, the photo-excited sensitizer (Dye*) is oxidized by the onium salt ($X-Y^+$) to form the corresponding radical cation (Dye$^{•+}$) and onium salt radical ($X-Y^•$), which then undergoes cleavage as depicted in Scheme 3. The radical, $Y^•$, may initiate free radical polymerization reactions, such as the polymerization of acrylate, while the radical cation, Dye$^{•+}$, may initiate the cationic polymerization of appropriate monomers. Alternatively, the radical cation may interact with solvents or monomers resulting in the release of strong protic acid, which similarly initiates cationic polymerization.

Photoinitiator systems that respond to visible light have been created in which perylene [5], cyanine [6], coumarin [7], acridinedione [8], or curcumin [9] dyes were used as sensitizers. These systems were applied to initiate both free radical [6–8] and cationic photopolymerization reactions [5,7,9]. Visible-light initiator systems are used in the fabrication of pigmented coatings, sunlight curing of water-based latex paints, curing of inks, and high-speed laser imaging [10].

Recent studies revealed that fluoflavin dyes [11] sensitized pyridinium salts to decomposition and that these photoredox pairs

* Fax: +48 42 636 25 96.
  E-mail address: radekpod@p.lodz.pl
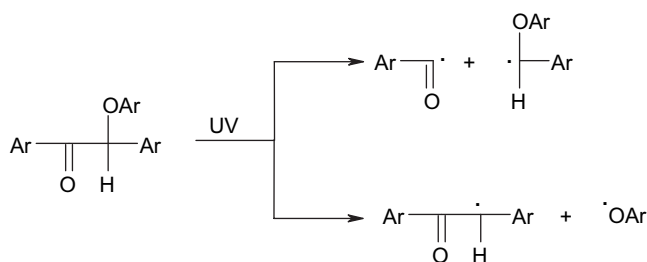
Scheme 1.

could efficiently initiate the polymerization of acrylate and tri-acrylate monomers. The main goals of this study were to synthesize novel dyes (**4a–4i**) based on the 5,12-dihydroquinoxalino[2,3-b]pyridopyrazine skeleton and to evaluate these dyes' spectroscopic, photophysical, and electrochemical properties. This paper also reports the application of this collection of dyes, **4**, as visible-light sensitizers for onium salts, such as N-methoxy-4-phenyl-pyridinium tetrafluoroborate (**Py1**), N-ethoxy-2-methylpyridinium hexafluorophosphate (**Py2**) and diphenyliodonium hexafluorophosphate (**Ph₂I**). Finally, experiments demonstrated that these new photooxidizable sensitization systems could be used as visible-light photoinitiators for free radical polymerization of acrylate monomers or for the cationic polymerization of cyclohexene oxide (CHO).
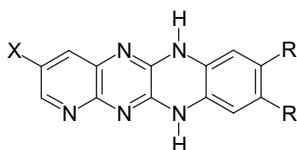
	X	R
4a	H	H
4b	H	CH₃
4c	H	Cl
4d	Br	H
4e	Br	CH₃
4f	Br	Cl
4g	Cl	H
4h	Cl	CH₃
4i	Cl	Cl

2. Experimental

2.1. General

Py1, **Ph₂I**, and the necessary synthesis reagents were purchased from Aldrich (Poznan, Poland) and Alfa Aesar (Gdansk, Poland). The final dyes were identified and characterized via ¹H NMR spectroscopy [Bruker Avance DPX 250, DMSO-d_6, TMS standard, δ (ppm)]. Their purity was also checked using TLC [Merck Silica gel 60, solvent: 3:1 (v/v) toluene/pyridine]. Absorption and steady-state fluorescence spectra were recorded using a Lambda 40 spectrophotometer (Perkin Elmer, USA) and a FluoroLog 3 spectrofluorimeter (Horiba Jobin Yvon, USA), respectively.

2.2. Synthesis

2.2.1. Synthesis of 7-bromo-2,3-(1H,4H)-pirydo-[2,3-b]-pyrazinodione (2b) [12]

5-Bromo-2,3-diaminopyridine (97%, 7.748 g, 0.04 mol) and oxalic acid (5.04 g, 0.04 mol) were refluxed in hydrochloric acid (30%, 40 ml) for 15 h. After cooling, the resulting precipitate was filtered and washed with water to give **2b** (6.83 g, 68%, m.p. > 360 °C), which was carried on to the next step of the synthesis without purification. The other pyrazinodiones, **2a** and **2c**, were synthesized in a similar fashion from the appropriate diaminopyridine starting material.

2.2.2. Synthesis of 7-bromo-2,3-dichloropyridopyrazine (3b) [13]

DMF was added dropwise (0.5 ml) to a solution of **2b** (6.8 g, 0.02 mol) in thionyl chloride (120 ml). The reaction mixture was refluxed for 15 h and then concentrated under vacuum. The resulting residue was coevaporated with chloroform several times, dissolved in chloroform (100 ml), and poured over ice-water. The organic layer was collected, washed with saturated aqueous NaCl, dried over Na₂SO₄, and then evaporated to provide **3b** as a brown solid (4.0 g, 50%), which was used for the next step in the synthesis without further purification. The other dichloropyridopyrazines, **3a** and **3c**, were synthesized in the same manner from the substrates **2a** and **2c**, respectively.

2.2.3. Synthesis of 9-bromo-5,12-dihydroquinoxalino [2,3-b]pyridopyrazine (4d) [14]

7-Bromo-2,3-dichloropyridopyrazine (1.3 g, 0.0047 mol) and o-phenylenediamine (1.01 g, 0.0094 mol) were refluxed in ethylene glycol (20 ml) for 2 h. After cooling, the orange precipitate was filtered, washed with methanol, dried, and recrystallized from acetic acid. The product (1.15 g) was obtained with a 78% yield. The other dyes were synthesized in the same manner from the appropriate o-phenylenediamines. Yield and ¹H NMR data for all the dyes are presented in Table 1.

2.2.4. Synthesis of N-ethoxy-2-methylpyridinium hexafluorophosphate [15]

2-Methylpyridine N-oxide (1.09 g, 0.01 mol) and triethyloxonium hexafluorophosphate (2.98 g, 0.012 mol) were refluxed in chloroform (3 ml) for 0.5 h. The crystalline product was recrystallized twice from ethanol.

M.p. 89 °C; ¹H NMR: 1.50 (t, J = 7.00, 3H), 2.85 (s, 3H), 4.62 (q, J = 7.00, 2H), 7.91–8.01 (m, 2H), 8.38 (td, J_1 = 1.25, J_2 = 6.50, 1H), 9.00 (dd, J_1 = 1.25, J_2 = 6.50, 1H).

### 2.3. Photochemical experiments

All photochemical experiments were carried out in a Rayonet Reactor RPR 200 (The Southern New England Ultraviolet Co, USA) equipped with eight lamps emitting light at 419 nm. Illumination intensity was measured using uranyl oxalate actinometry [16].

The fluorescence quantum yield of the dye (Φ_{dye}) was calculated from the following equation:

X⁻ = PF₆⁻, SbF₆⁻, AsF₆⁻, etc.

Scheme 2.

$$\Phi_{dye} = \Phi_{ref} I_{dye} A_{ref} n_{dye}^2 / I_{ref} A_{dye} n_{ref}^2 \tag{1}$$
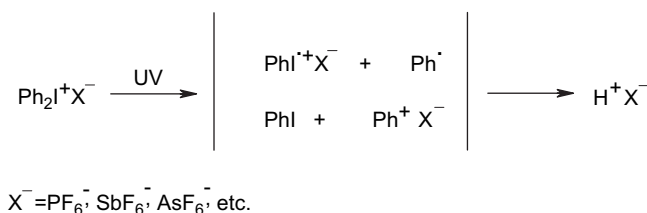
Scheme 3.
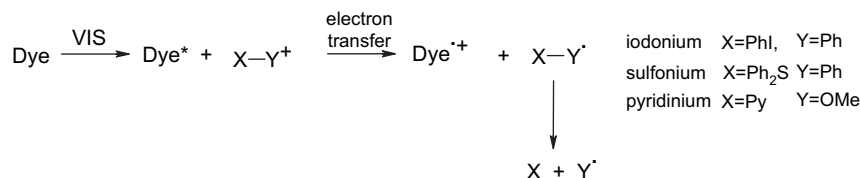
in which Φ_{ref} denotes the fluorescence quantum yield of the 5,12-dihydroquinoxalino[2,3-b]quinoxaline reference ($\Phi_{ref} = 0.8$ in 1-methyl-2-pyrrolidone [11]), A_{dye} and A_{ref} denote the absorbances of the dye and the reference at the excitation wavelengths (410 nm), I_{dye} and I_{ref} refer to the areas under the fluorescence peaks of the dye and reference, and n_{dye} and n_{ref} are the solvent refractive index for the dye and reference, respectively.

Free radical photopolymerization reactions were conducted in solvents composed of 1 ml of 1-methyl-2-pyrrolidone (MP) and 4 ml of methyl acrylate (MeAc) or trimethylolpropane triacrylate (TMPTA). Dye concentration was maintained at 0.1 mM, and the concentration of alkoxypyridinium salts was 10 mM. The rate of polymerization (R_p) was calculated from Eq. (2), where Q_s is the heat flow per second during the reaction, m is the mass of the monomer in the sample, M is the molar mass of the monomer, n is the number of double bonds per monomer, and ΔH_p is the theoretical enthalpy for complete polymerization of acrylate double bonds (20.6 kcal mol^{-1}) [17].

$$R_p = Q_s \cdot M / n \cdot \Delta H_p \cdot m \qquad (2)$$

A PT 401 temperature sensor (Elmetron, Poland) was immersed in the sample to measure heat flow. The conversion of MeAc into poly(MeAc) after 2 min of irradiation was determined gravimetrically.

Cationic photopolymerization was conducted in cyclohexene oxide (5 ml) solvent under an N$_2$ atmosphere. The concentrations of the dye and diphenyliodonium salt were 0.1 mM and 10.0 mM, respectively. CHO was polymerized using a 30-min exposure to radiation, and the resulting solution was poured into 50 ml of methanol containing roughly 1 ml of NH$_3$ (30%). The precipitated polymers were isolated by filtration, washed with cold methanol, and dried overnight in a vacuum oven at 45 °C. The conversion of CHO into poly(CHO) was then determined gravimetrically.

The quantum yield of sensitized proton formation $\Phi(H^+)$ was determined using sodium bromophenol blue (BPhBl), which demonstrated a vanishing peak absorbance at 606 nm during irradiation. The proton concentration was estimated from the calibration curve of the BPhBl optical density vs. water-free hexafluoroantimonic acid. The $\Phi(H^+)$ was calculated from at least three separate measurements of reactions that were $14 \pm 3\%$ complete.

The quantum yield of singlet oxygen formation $\Phi(^1O_2)$ and electrochemical experiments was measured as described in Ref. [11].
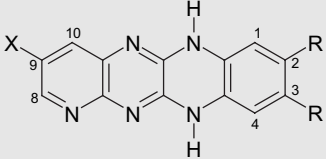
3. Results and discussion

3.1. Synthesis and spectroscopic characterization of dyes

The synthesis of the collection of dyes, **4**, is outlined in Scheme 4. In the first step, the corresponding diaminopyridines (**1a**–**c**) were cyclized with oxalic acid in refluxing hydrochloric acid (30%) to give the corresponding derivatives of 2,3-(1H,4H)-pirydo-[2,3-b]-pyrazinodione (**2a**–**c**) in 70% yield [12]. The chlorination of **2** by treatment with thionyl chloride provided 2,3-dichloropyridopyrazines [13], **3a**–**c**, in 50–56% yield. Finally, dyes **4a**–**4i** were synthesized by refluxing **3a**–**c** with the appropriate symmetric o-phenylenediamines in ethylene glycol [14].

The crude dyes were purified by recrystallization from acetic acid until a constant molar excitation coefficient and TLC purity were obtained. Dyes **4** were synthesized in excellent 78–98% yield, and their chemical structures were verified by ^{1}H NMR (Table 1). The spectroscopic properties (absorption and fluorescence) of dyes **4a**–**4i** are presented in Table 2. Dyes **4** had absorption bands in the visible region located at approximately 415 nm and strong emission bands characterized by an ≈ 63–69 nm Stokes shift. These values indicated that the geometry of the singlet excited state does not differ greatly from the geometry of the ground state [18]. The

Table 1
Yield and ^{1}H NMR spectra of dyes **4a**–**4i**

Dye	Yield	^{1}H NMR
4a	81	6.76–6.81 (m, 2H, H1,H4), 6.98–7.20 (m, 4H, H2,H3,H9,H10), 7.71–7.84 (m, 1H, H8) 11.11 (bs, 2H, NH)
4b	96	1.97 (s, 6H, CH₃), 6.73 (s, 2H, H1,H4), 6.87–6.89 (m, 3H, H8,H9,H10), 7.57 (bs, 2H, NH)
4c	98	6.76–6.81 (1H, m, H1), 6.95–6.97 (1H, m, H4), 7.22–7.43 (m, 3H, H8,H9,H10), 7.68 (bs, 2H, NH)
4d	78	6.97–7.04 (m, 4H, H1,H2,H3,H4), 7.20 (s, 2H, H8,H10), 7.85 (s, 2H, NH)
4e	84	1.91 (s, 6H, CH₃), 6.77 (m, 2H, H1,H4), 6.98 (s, 1H, H10), 7.65 (s, 1H, H8), 12.01 (bs, 2H, NH)
4f	86	3.59 (bs, 2H, NH), 7.05–7.13 (m, 2H, H1,H4), 7.73 (s, 1H, H10), 7.91 (s, 1H, H8)
4g	81	6.97–7.04 (m, 4H, H1,H2,H3,H4), 7.10 (s, 2H, H8,H10), 7.80 (s, 2H, NH)
4h	85	2.20 (s, 6H, CH₃), 6.85 (s, 2H, H1,H4), 6.95 (s, 1H, H10), 7.66 (s, 1H, H8), 11.78 (bs, 2H, NH)
4i	89	7.03 (s, 2H, H1,H4), 7.20 (s, 1H, H10), 7.74 (s, 1H, H8), 11.8 (bs, 2H, NH)
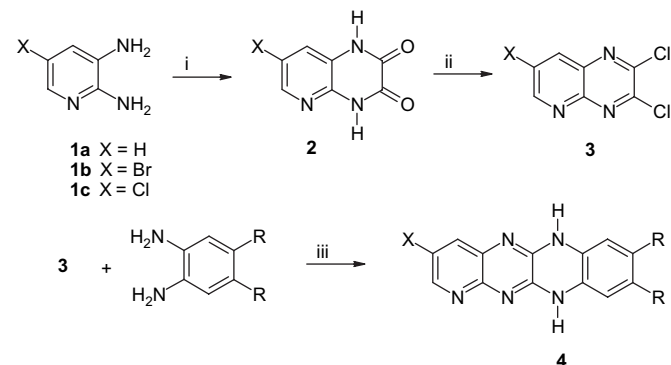
Scheme 4. (i) Oxalic acid, 30% HCl; (ii) SOCl$_2$, DMF; (iii) ethylene glycol.

Table 2
Spectroscopic, photophysical, and electrochemical parameters of the examined dyes

Dye	λ_c^a [nm]	$\lg \varepsilon^a$	λ^b [nm]	λ_{fl}^b [nm]	Φ_{fl}^b	Stokes shift [nm]	$\Phi(^1O_2)^a$	E_{ox} [V]^c	E^{00} [kJ mol^{-1}]
4a	411	4.25	406	470	0.39	64	0.10	0.44	275.8
4b	413	4.29	409	478	0.42	69	0.10	0.36	273.9
4c	420	4.34	417	486	0.48	69	0.14	0.60	268.4
4d	409	4.36	406	469	0.29	63	0.50	0.53	273.3
4e	414	4.29	410	479	0.16	69	0.31	0.46	271.4
4f	421	4.42	417	486	0.18	69	0.28	0.68	267.8
4g	409	4.32	406	469	0.62	63	0.17	0.57	275.8
4h	414	4.27	410	476	0.63	66	0.18	0.39	273.3
4i	421	4.37	416	484	0.42	68	0.19	0.65	268.4

^a In 1-methyl-2-pyrrolidone.
^b In cyclohexene oxide.
^c In DMF.

[a] In 1-methyl-2-pyrrolidone.
[b] In cyclohexene oxide.
[c] In DMF.

electronic absorption (UV–vis) and emission spectra of dye **4c** are presented in Fig. 1. For all dyes tested, the absorption and fluorescence spectra were nearly mirror images of each other with overlapping bands corresponding to the $0 \rightarrow 0$ transition. The absorption spectra were typical of those of polycyclic aromatic heterocycles, which have a characteristic vibrational structure. In comparison with 5,12-dihydroquinoxalino[2,3-*b*]quinoxaline [11], the presence of an additional nitrogen in 5,12-dihydroquinoxalino[2,3-*b*]pyridopyrazine caused a small hypsochromic effect (6 nm). Moreover, the position of the absorption band depended on the character of a dye's R group. For dyes **4a**, **4d**, and **4g**, the absorption bands were located at approximately 410 nm. The presence of two methyl substituents (**4b**, **4e**, and **4h**) caused a red-shift in the absorption band compared to the corresponding unmethylated dye. A larger bathochromic effect was observed for dyes **4c**, **4f**, and **4i**. In these dyes, the absorption bands were located at approximately 420 nm. Additionally, the character of the X substituent had no effect on the position of these molecules' absorption bands. The examined dyes exhibited small solvatochromic effects. A bathochromic shift between the nonpolar solvent (cyclohexene oxide, $\varepsilon \approx 9$) and polar solvents (1-methyl-2-pyrrolidone, $\varepsilon = 33$) of only 4–5 nm was observed.

The fluorescence quantum yields (Φ_{fl}) of dyes are presented in Table 2. As can be seen from these data, the Φ_{fl} of these dyes range from 0.16 to 0.63 with dyes **4d**–**4f** having the smallest values of Φ_{fl}. Adding heavy atoms such as Br to a fluorescent system is known to

stabilize a molecule's triplet state, because this increases the efficiency of the intersystem crossing process. In order to clarify the photochemistry of dyes **4a**–**4i**, their quantum yields of singlet oxygen generation [$\Phi(^1O_2)$] were measured in an oxygen-saturated solution (Table 2). In accordance with the aforementioned heavy atom effects, the quantum yield of singlet oxygen generation was much higher for the dyes derived from 7-bromo-2,3-dichloropyridopyrazine.

### 3.2. Free radical and cationic photopolymerization

Spectroscopic studies revealed that the dyes **4** could be applied as visible sensitizers for the collection of light > 400 nm. The well-known mechanism of the dye-sensitized photodecomposition of onium salts [4–6] is presented in Scheme 3. Irradiation of these photoredox pairs leads to electron transfer from the excited sensitizer (Dye*) to the onium salt (X–Y$^+$). The resulting onium radical (X–Y$^•$) is then cleaved to yield the initiator radical ($^•$Y), sensitizer radical cation (Dye$^{•+}$) and neutral molecule X. N-alkoxypyridinium salt cleavage yields pyridine and an alkoxy radical, while diphenyliodonium salt cleavage yields iodobenzene and a phenyl radical.

The free energy change of the photoinduced electron transfer from the excited dyes **4** to the onium salt employed in this study was calculated from the Rehm–Weller equation as follows (Eq. 3) [19]:

$$\Delta G_{et}\left(kJmol^{-1}\right) = 97\left[E_{ox}\left(S/S^{•+}\right) - E_{red}\left(A^{•-}/A\right)\right] - Ze^2/\varepsilon a - E^{00}(S) \tag{3}$$

In this equation, E_{ox} (S/S$^{•+}$) and E_{red} (A$^{•-}$/A) are the oxidation potential of the dye (**4**) and the reduction potential E_{red} (A$^{•-}$/A) of the onium salt, respectively. The $E^{00}(S)$ is the singlet excited state energy of the dye (**4**), which is given in Table 2. In this calculation, the Coulombic energy, $Ze^2/\varepsilon a$, was omitted, because the dye **4**/onium salt system employed involved photoredox pairs without electrostatic interactions both in the ground state and after electron transfer.

In order to be able to calculate ΔG_{et}, the oxidation potentials of dyes **4** were measured in separate experiments. The cyclic voltammogram of dye **4c** is presented in Fig. 2, and the measured oxidation potentials (E_{ox}) of all of the dyes are presented in Table 2. In all cases, the electrochemical oxidation was irreversible, and the location of the oxidation peak depended on the structure of the dye.
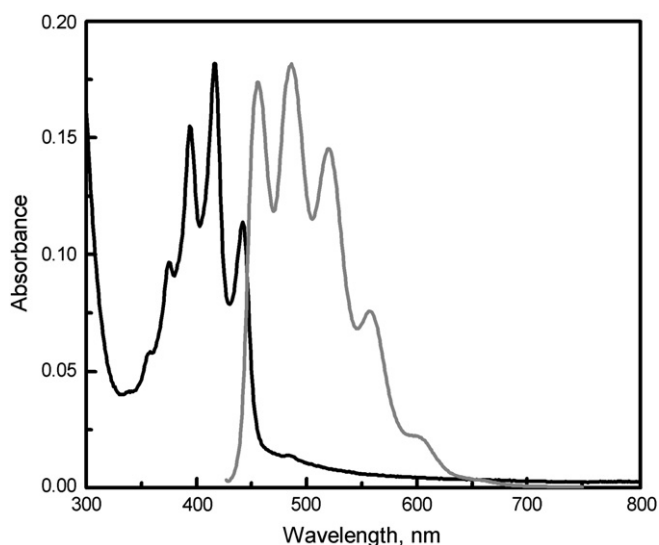
Fig. 1. Normalized absorption (black) and emission (gray) spectra of dye **4c** (8 μM) in cyclohexene oxide.
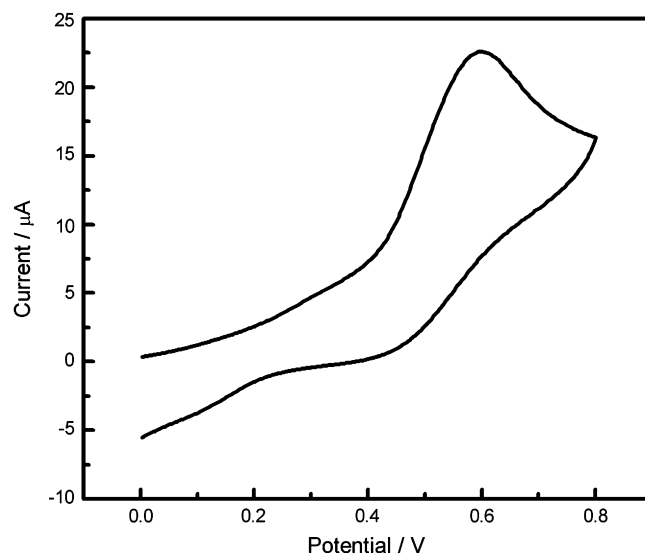
Fig. 2. Cyclic voltammogram of dye **4c** in DMF. Scan rate: 0.1 V s^{-1}.

Table 3
Thermodynamic data (kJ mol^{-1})

Dye	ΔG_{el}[a]	ΔG_{el}[b]	ΔG_{el}[c]
4a	−133.7	−114.3	−162.8
4b	−139.5	−120.1	−168.7
4c	−110.8	−91.4	−139.9
4d	−122.5	−103.1	−151.6
4e	−127.3	−107.9	−156.4
4f	−102.4	−83.0	−131.5
4g	−121.1	−101.7	−150.2
4h	−136.0	−116.6	−165.1
4i	−105.9	−86.5	−135.0

[a] With Py1 (E_{red}: −1.025 V).
[b] With Py2 (E_{red}: −1.225 V).
[c] With Ph$_2$I (E_{red}: −0.725 V); E_{red} from Ref. [20].

The results indicated that dyes with two methyl groups (**4b**, **4e**, and **4h**) are more readily oxidized than both unsubstituted dyes (**4a**, **4d**, and **4g**) and halogen-substituted analogues (**4c**, **4f**, and **4i**). Moreover, dyes **4a–4c** were oxidized at a lower potential compared to the halogen-substituted dyes, **4d–4i**.

Once the E_{ox} and E^{00} values of the dyes, **4**, and the reduction potential of the onium salt [20] had been measured, the ΔG_{et} could be calculated using Eq. (3). The calculated thermodynamic parameters listed in Table 3 indicated that all the tested dye/onium systems possed a high, favorable thermodynamic driving force upon exposure to light ($-\Delta G_{et} > 83$ kJ mol^{-1}). This meant that the excited state photoelectron transfer was quite facile.

Finally, the dye/pyridinium photoredox pairs were examined for potential applications as initiators for the free radical polymerization of methyl acrylate (MeAc) and trimethylolpropane triacrylate (TMPTA) monomers. The efficiency of the polymerization initiated by the **4**/Py1 and **4**/Py2 systems was measured indirectly from the reaction's heat flow during irradiation (Fig. 3). In the case of MeAc polymerization, the polymerization reaction was also observed to proceed after the termination of irradiation. The overall polymerization results are summarized in Table 4.

The calculated polymerization rate (R_p) and the final conversion of MeAc (Table 4) indicated that the efficiency of polymerization strongly depended upon the structure of the dye employed. It was apparent that dyes **4d–4f** significantly accelerated both acrylate and triacrylate photopolymerization. It is well-known that the rate

Table 4
Rate of photopolymerization (μmol s^{-1}), inhibition time (s) and conversion (%) of monomers

| Dye	TMPTA				MeAc[a]				CHO[a]	MP[a]
	Py1		Py2		Py1		Py2		Ph$_2$I	
	R_p	Inhibition time	R_p	Inhibition time	R_p	%	R_p	%	%	Φ(H$^+$) × 10^{-3}
4a	23.9[a]	–	25.1[a]	–	23.0	24	29.0	36	6	0.97
4b	24.4[a]	–	28.5[a]	–	22.7	31	30.8	41	2	0.25
4c	27.5	99	39.1	91	25.0	32	30.3	23	3	0.38
4d	81.2	14	84.3	60	55.3	38	48.0	41	37	7.16
4e	74.7	64	85.3	62	48.3	50	42.2	44	22	3.31
4f	73.5	35	82.8	47	40.8	38	45.2	47	46	8.34
4g	54.3	80	58.5	89	36.6	31	34.6	45	33	5.88
4h	59.3	82	40.5	88	38.7	44	32.0	44	20	2.88
4i	48.8	77	42.7	79	33.4	45	33.6	19	23	3.94

[a] N$_2$ atmosphere.

of the photoinitiated polymerization depends on the efficiency of the excited triplet state formation [21] as shown in Eq. (4):

$$R_p = k_p[M](I_a \Phi_T k_{el}/k_t)^{0.5} \tag{4}$$

in which I_a is the intensity of the absorbed light, Φ_T is the quantum yield of triplet state formation, k_p and k_t denote the rate constants of polymerization and chain termination steps, respectively, and k_{el} is the first-order rate constant of the electron transfer. The relationship between R_p and the square root of $\Phi(^1O_2)$ (Fig. 4) revealed the possibility that the electron transfer between dyes and the pyridinium salt occurs via the triplet state [11,21].

The free radical polymerization initiated by tested photoredox pairs showed a significant inhibition period (Fig. 3 and Table 4). This effect should be related to the molecular oxygen dissolved in the composition. The oxygen both quenches the triplet state of the dye and reacts with radical species generated by the dye/pyridinium salt systems. After the consumption of the oxygen, the initiating radicals react with the monomer. The relationship between the polymerization rates and the inhibition times (Fig. 5) revealed that the most efficient photoredox pair has the shortest inhibition time [22].

The dye **4**/Ph$_2$I photoredox pairs were also examined for their usefulness as photoinitiators for the cationic polymerization of
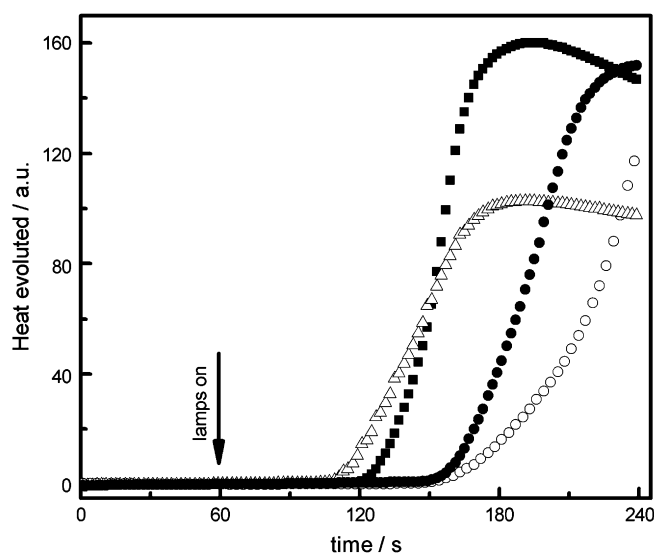
Fig. 3. Kinetic curves of TMPTA photopolymerization recorded under an air atmosphere for Py2 and dyes **4c** (○); **4d** (■); **4g** (●); **4f** (△).
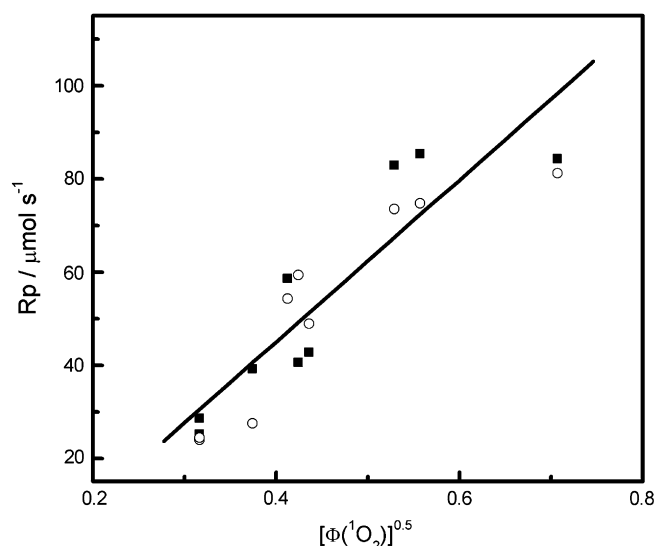
Fig. 4. Relationship between the rate of polymerization initiated by dye/Py1 (○) and dye/Py2 (■) systems and the square root of the quantum yield of singlet oxygen formation.
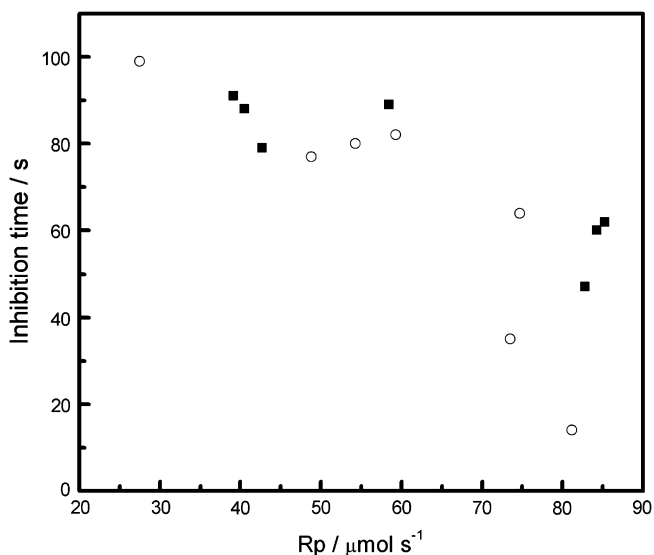
Fig. 5. Relationship between inhibition time and the rate of photoinitiated polymerization initiated by dye/**Py1** (○) and dye/**Py2** (■) systems.

Fig. 7. Relationship between the quantum yield of acid release and the conversion of CHO.

cyclohexene oxide (CHO). For these experiments, polymerization was conducted under an N_2 atmosphere, and the reaction mixture was irradiated for 30 min. The details regarding the conversion of CHO into poly(CHO) are presented in Table 4. It was evident that dyes **4d–4i** significantly accelerated CHO polymerization.

It is well-known that protic acids initiate cationic polymerization reactions [3–5]. In order to confirm the formation of the acid during photolysis of the **4**/**Ph₂I** systems, the quantum yield of acid release [$\Phi(H^+)$] upon photolysis was measured using sodium bromophenol blue (BPhBl). The quantity of acid released was estimated using a calibration curve relating the BPhBl absorbance as a function of $HSbF_6$ concentration (inset Fig. 4). In all the dye/**Ph₂I** combinations studied, the solution acidity increased over time as the solution was irradiated, and so the solution's BPhBl absorbance at λ_{max} (606 nm) decreased correspondingly (Fig. 6). In contrast, photolysis of the dyes alone did not change the solution pH. The
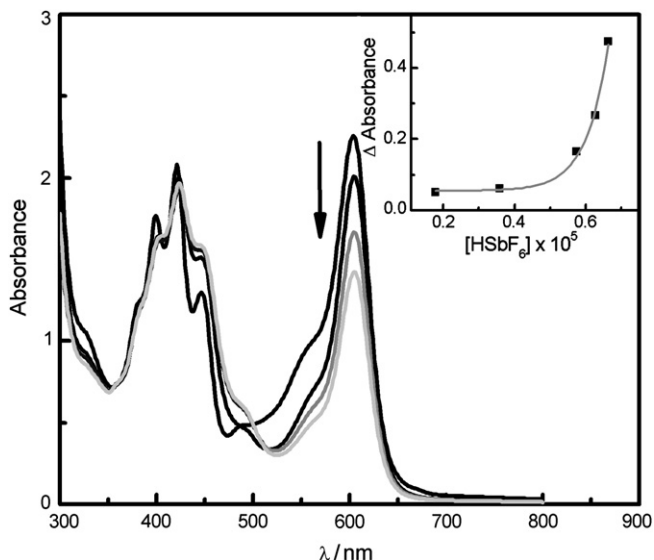
calculated quantum yields of acid release are presented in Table 4. Dye **4f** demonstrated the highest quantum yield of acid release. Moreover, there was a linear relationship between $\Phi(H^+)$ and the conversion of CHO (Fig. 7). This suggested that the proton, formed upon photolysis of the **4**/**Ph₂I** systems, was the crucial species necessary for initiating the cationic polymerization of CHO.

It was apparent that the dyes **4d–4f** significantly accelerated the photopolymerization of acrylate and epoxide monomers. These compounds also had the highest quantum yields of singlet oxygen generation (Table 2). The relationships between the square root of $\Phi(^1O_2)$ and the rate of free radical polymerization and $\Phi(^1O_2)$ and the conversion of CHO revealed the possibility that the oxidation of dyes **4d–4f** may occur via the triplet state [11,21].

4. Conclusions

Novel dyes based on the 5,12-dihydroquinoxalino[2,3-*b*]pyridopyrazine skeleton were successfully synthesized and characterized using ^{1}H NMR spectroscopy. These new dyes, when combined with onium salts such as *N*-methoxy-4-phenylpyridinium tetrafluoroborate (**Py1**), *N*-ethoxy-2-methylpyridinium hexafluorophosphate (**Py2**), or diphenyliodonium hexafluorophosphate (**Ph₂I**), may have practical applications as visible-light photoinitiators of free radical and/or cationic polymerization. The ability of each individual dye to act as a photoinitiator strongly depended upon its unique chemical structure. Furthermore, the heavy atoms present in dyes **4d–4f** could promote the formation of the dyes' excited triplet states, thereby facilitating electron transfer from these triplet states.

Fig. 6. Electronic absorption spectra obtained upon photolysis (time interval, 15 s) of an N_2-saturated solution of BPhBl (20 μM) and dye **4f** (0.1 mM)/**Ph₂I** (1.0 mM) system in 1-methyl-2-pyrrolidone. Inset: calibration curve of change in BPhBl (20 μM) absorbance vs. $HSbF_6$ concentration (range 0–70 μM).
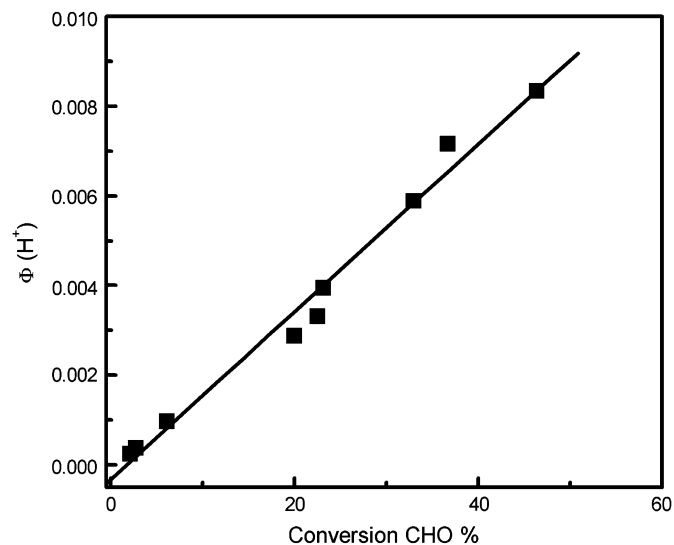
References

[1] Fouassier JP. In: Fouassier JP, Rabek J, editors. Radiation curing in polymer science and technology vol. 1. London: Elsevier; 1993. p. 49–113.
[2] Allen NS. Photoinitiators for UV and visible curing of coatings: mechanisms and properties. J Photochem Photobiol A: Chem 1996;100:101–9.
[3] Crivello JV. The discovery and development of onium salt cationic photoinitiators. J Polym Sci A Polym Chem 1999;37:4241–54.

[4] Selvaraju C, Sivakumar A, Ramamurthy P. Excited state reactions of acridine-dione dyes with onium salts: mechanistic details. J Photochem Photobiol A: Chem 2001;138:213–26.

[5] Neumann MG, Rodriques MR. A study of the elemental reactions involved in the initiation of the polymerization of tetrahydrofuran induced by the photosensitization of a triphenylsulphonium salt by perylene. J Braz Chem Soc 2003;14:76–82.

[6] Gould IR, Shukla D, Giesen D, Farid S. Energetics of electron-transfer reactions of photoinitiated polymerization: dye-sensitized fragmentation of N-alkoxypyridinium salts. Helv Chim Acta 2001;84:2796–812.

[7] Zhu QQ, Schnabel W. Cationic photopolymerization under visible laser light: polymerization of oxiranes with coumarin/onium salt initiator systems. Polymer 1996;37:4129–33.

[8] Timpe HJ, Urlich S, Decker C, Fouassier JP. Photoinitiated polymerization of acrylates and methacrylates with decahydroacridine-1,8-dione/onium salt initiator systems. Macromolecules 1993;26:4560–6.

[9] Crivello JV, Bulut U. Curcumin: a naturally occurring long-wavelength photosensitizer for diaryliodonium salts. J Polym Sci A Polym Chem 2005;43:5217–31.

[10] Fouassier JP, Allonas X, Burget D. Photopolymerization reactions under visible lights: principle, mechanisms and examples of applications. Prog Org Coat 2003;47:16–36.

[11] Podsiadły R. Photoreaction and photopolymerization studies on fluoflavin dye-pyridinium salt systems. J Photochem Photobiol A: Chem 2008; 198:60–8

[12] Ohmori J, Kubota H, Shimizu-Sasamata M, Okada M, Sakamoto S. Novel α-amino-3-hydroxy-5-methylisoxazole-4-propionate receptor antagonists: synthesis and structure–activity relationships of 6-(1H-imidazol-1-yl)-7-nitro-2,3(1H,4H)-pyrido[2,3-b]pyrazinedione and related compounds. J Med Chem 1996;39:1331–8.

[13] Ohmori J, Shimizu-Sasamata M, Okada M, Sakamoto S. 8-(1H-imidazol-1-yl)-7-nitro-4(5H)-imidazo[1,2-a]quinoxalinone and related compounds: synthesis and structure–activity relationships for the AMPA-type non-NMDA receptor. J Med Chem 1997;40:2053–63.

[14] Hunig S, Scheutzow D, Schlaf H, Quast H. Synthese heterocyclish tetrsubstituierter Äthylene und ihrer höheren Oxidationsstufen. Liebigs Ann Chem 1972;765:110–25.

[15] Reichardt C. Notiz zur Darstellung von N-Äthoxy-pyridinium- und –chinolinium salzen. Chem Ber 1966;97:1769–70.

[16] Leighton WB, Forbes GS. Precision actinometry with uranyl oxalate. J Am Chem Soc 1930;52:3139–52.

[17] Avci D, Nobles J, Mathias LJ. Synthesis and photopolymerization kinetics of new flexible diacrylate and dimethacrylate crosslinkers based on C18 diacid. Polymer 2003;44:963–8.

[18] Bojinov VB, Panova IP, Grabchev IK. Novel polymerizable light emitting dyes – combination of a hindered amine with a 9-phenylxanthene fluorophore. Synthesis and photophysical investigations. Dyes Pigments 2007;74:187–94.

[19] Rehm D, Weller A. Kinetics of fluorescence quenching by electron and H-atom transfer. Isr J Chem 1970;8:259–71.

[20] Schnabel W. Cationic photopolymerization with the aid of pyridinium-type salts. Macromol Rapid Comm 2000;21:628–42.

[21] Przyjazna B, Kucybała Z, Pączkowski J. Development of new dyeing photoinitiators based on 6H-indolo[2,3-b]quinoxaline skeleton. Polymer 2004;45:2559–66.

[22] Neumann MG, Schmitt CC, Goi BE. The mechanism of the photoinitiation of methyl methacrylate polymerization by the neutral red/triethylamine system. J Photochem Photobiol A: Chem 2005;174:239–45.